Inorganic Chemistry

pubs.acs.org/IC

Article

Rhenium Corrole Dimers: Electrochemical Insights into the Nature of the Metal−Metal Quadruple Bond

Abraham B. Alemayehu, Laura J. McCormick-McPherson, Jeanet Conradie, and Abhik Ghosh*

Cite This: *Inorg. Chem.* 2021, 60, 8315−8321

Read Online

ACCESS | Metrics & More | Article Recommendations | Supporting Information

ABSTRACT: The interaction of free-base triarylcorroles with $Re_2(CO)_{10}$ in 1,2-dichlorobenzene in the presence of 2,6-lutidine at 180 °C under strict anerobic conditions afforded approximately 10% yields of rhenium corrole dimers. The compounds exhibited diamagnetic ^{1}H NMR spectra consistent with a metal−metal quadruple bond with a $\sigma^2\pi^4\delta^2$ orbital occupancy. One of the compounds proved amenable to single-crystal X-ray structure determination, yielding a metal−metal distance of ∼2.24 Å, essentially identical to that in triple-bonded osmium corrole dimers. On the other hand, the electrochemical properties of Re and Os corrole dimers proved to be radically different. Thus, the reduction potentials of the Re corrole dimers are some 800 mV upshifted relative to those of their Os counterparts. Stated differently, the Re corrole dimers are dramatically easier to reduce, reflecting electron addition to δ^* versus π^* molecular orbitals for Re and Os corrole dimers, respectively. The data also imply electrochemical HOMO-LUMO gaps of only 1.0−1.1 V for rhenium corrole dimers, compared with values of 1.85−1.90 V for their Os counterparts. These HOMO−LUMO gaps rank among the first such values reported for quadruple-bonded transition-metal dimers for any type of supporting ligand, porphyrin-type or not.

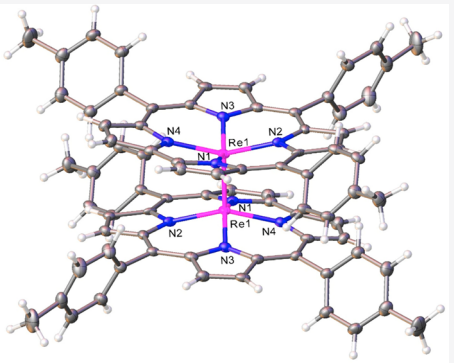

INTRODUCTION

The interpretation of the very short Re−Re distance in the $[Re_2Cl_8]^{2-}$ dianion[1,2] as indicative of a metal−metal quadruple bond by Cotton in 1965 stands as a landmark in the history of chemical bonding.[3−7] The novel feature of such a bond is a δ-orbital interaction, in addition to a σ and two π interactions. Subsequently, it became clear that the δ interaction makes only a small contribution to the metal−metal interaction energy and has next to no effect on the metal−metal distance.[8] Nevertheless, the δ interaction has major implications for many physicochemical properties and especially for redox chemistry. Many of these insights originated from Collman and Arnold's extensive studies of 4d and 5d metalloporphyrin dimers.[9] For example, temperature-dependent ^{1}H NMR studies of molybdenum and tungsten porphyrin dimers provided some of the first estimates of the strength of the δ interaction.[10−12] Likewise, resonance Raman studies of molybdenum, rhenium, and osmium porphyrin dimers provided some of the first insights into the vibrational characteristics of metal−metal multiple bonds.[13] Remarkably, in spite of sustained attention over decades, significant questions remain relative to the energetics of δ bonds. (a) How much are typical δ−δ^* transition energies, especially as a function of different metals? (b) How much are typical singlet−triplet gaps? (c) What about the electrochemical HOMO-LUMO gaps? The last, in theory, would appear to be a simple matter; in practice, few quadruple-bonded systems exhibit clean, reversible reductions in their cyclic voltammograms, thwarting a simple approach to answering the question. Here we report a new class of quadruple-bonded systems in the form of three rhenium *meso*-triarylcorrole dimers, one of which was characterized via single-crystal X-ray diffraction analysis. Electrochemical studies and density functional theory (DFT) calculations on the complexes have now provided some of the clearest answers yet to the above questions,[14,15] as outlined below.

RESULTS AND DISCUSSION

Synthesis and Proof of Structure. Ironically, given our long-standing interest in metal−metal multiple bonds,[16,17] we stumbled upon the first quadruple-bonded metallocorrole dimer through sheer serendipity. Attempted derivatization of an $ReCl_2$ Viking helmet corrole (generated as described by Bröring and co-workers[18]) with PhMgBr failed to yield the expected $RePh_2$ product; mass spectrometric (MS) analysis of the products instead showed the presence of small quantities of what appeared to be a rhenium corrole dimer (Scheme 1). A further lucky break came, even before spectroscopic data were

Received: March 30, 2021
Published: May 17, 2021

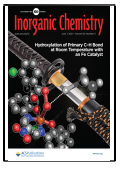

Scheme 1. Two Routes to Rhenium Corrole Dimers

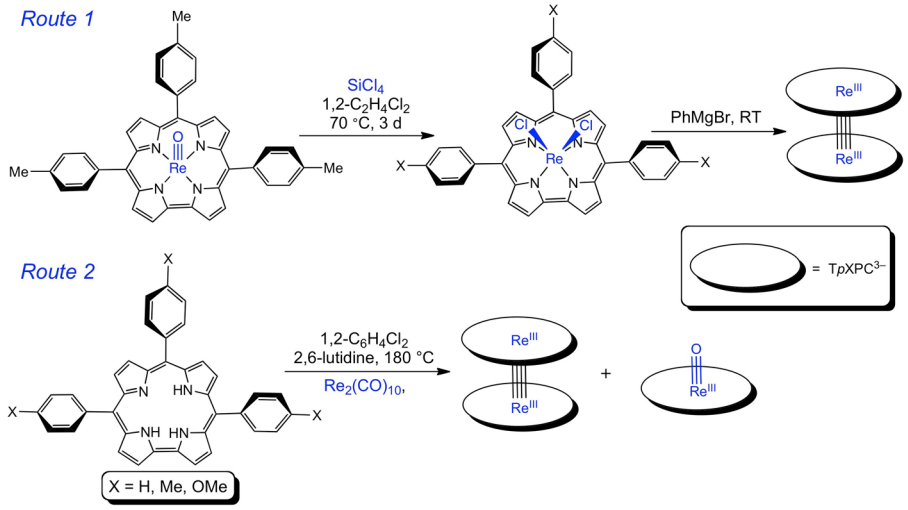

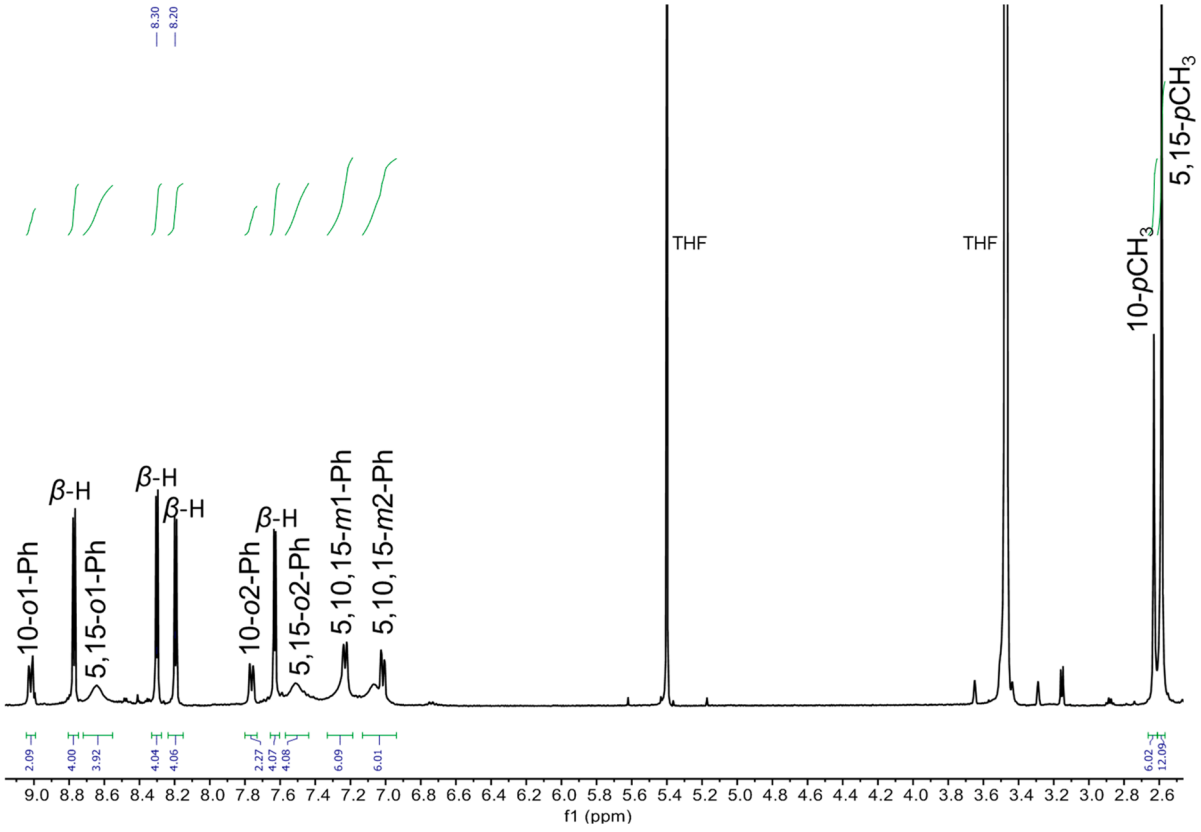

Figure 1. ^{1}H NMR spectrum of {Re[T*p*MePC]}$_2$ in THF-d_8 at 298 K.

in place, in the form of a single-crystal X-ray diffraction structure, providing definitive proof of the formation of a multiple-bonded metallocorrole dimer.

Understandably, we sought a more rational route to the novel product. The interaction of free-base *meso*-tris(*p*-X-phenyl)corroles,[19,20] H$_3$[T*p*CH$_3$PC] (X = H, Me, OMe), with Re$_2$(CO)$_{10}$ in 1,2-dichlorobenzene in the presence of 2,6-lutidine at 150 °C under strictly anerobic conditions yielded traces of the dimers {Re[T*p*XPC]}$_2$ along with significant amounts of Re[T*p*XPC](O),[21] the latter a testament to the exceedingly oxophilic nature of rhenium (Scheme 1). Increasing the temperature appeared to improve the yield of the dimer; ultimately, reflux conditions (i.e., a temperature of 180 °C) were considered optimum, which reliably led to >10% yields of the dimer. The Re corrole dimers could be readily separated from the ReO corroles via column chromatography so the synthesis, in spite of the low yields, proved simple and untedious in practice.

The Re corrole dimers yielded reasonably sharp ^{1}H NMR spectra at room temperature (Figure 1), providing unambiguous proof that the compounds are diamagnetic, consistent with a $\sigma^2\pi^4\delta^2$ quadruple-bonded description. The spectra could be essentially fully assigned, revealing symmetry-related *meso*-triarylcorrole ligands in which the ortho and meta protons of

https://doi.org/10.1021/acs.inorgchem.1c00986
Inorg. Chem. 2021, 60, 8315−8321

each phenyl ring are split into symmetry-distinct pairs, as is typical for square-pyramidally coordinated corrole derivatives.[21−24] Unfortunately, the complex temperature-dependent dynamic behavior of the compounds prevented us from investigating the energetics of corrole rotation about the metal−metal axis, as was previously accomplished for Mo and W porphyrin dimers.[10−12]

The X-ray structure of {Re[T*p*MePC]}$_2$ (space group *Pbcn*; Table 1 and Figure 2) indicated a dimer conformation with a crystallographically imposed center of symmetry: the preference for such a conformation is readily understandable in that it averts steric interactions between the 10-aryl groups. The metal−metal distance was found to be 2.236 Å, essentially identical with that found for Os corrole dimers.[17] The distance is also very close to twice Pyykkö's triple-bond covalent radius for Re (1.10 Å),[25] proving (as elsewhere in the literature[7,9]) that the δ bond has little impact on the metal−metal distance. In other respects, the coordination geometry is unremarkable, with metal−nitrogen distances hovering around 2.00 Å, essentially the same as those in ReO corroles and a couple of hundredths of an angström longer than those in Os corrole dimers.[17] Finally, the Re atom in {Re[T*p*MePC]}$_2$ is displaced by about 0.531 Å above the mean N_4 plane of the corrole, comparable to the analogous displacement of the metal in ReO[21] and OsN[26] corroles as well as in Os corrole dimers.[17]

Table 1. Crystallographic Data for {Re[T*p*CH$_3$PC]}$_2$

chemical formula	$C_{82}H_{62}N_8Cl_4Re_2$
formula mass	1673.59
crystal system	orthorhombic
crystal size (mm^3)	0.520 × 0.060 × 0.030
space group	*Pbcn*
λ (Å)	0.7749
a (Å)	14.9614(9)
b (Å)	20.5775(13)
c (Å)	21.8546(13)
α (deg)	90
β (deg)	90
γ (deg)	90
Z	4
V (Å^3)	6728.3(7)
temperature (K)	100(2)
density (g/cm^3)	1.652
no. of measured reflns.	368715
no. of unique reflns.	8721
no. of parameters	436
no. of restraints	0
R_{int}	0.0772
θ range (deg)	2.032−31.617
R_1, wR_2 all data	0.1094, 0.2288
S (GOF) all data	1.077
max/min residual density (e/Å^3)	3.026/−2.096

UV−Vis Spectroscopy and Electrochemistry. The optical spectra of the Re corrole dimers (Table 2 and Figure 3) proved rather unremarkable and qualitatively similar to those of their Os counterparts, with reasonably sharp Soret (405−408 nm) and Q (599−602 nm) bands. These are, however, hypsochromically and bathochromically shifted respectively relative to the main Soret (439−441 nm) and Q (585−592 nm) bands of the corresponding ReO corroles.[21] No near-IR bands were evident up to 1200 nm.

Cyclic voltammetry, on the other hand, uncovered major differences among Re, Ru,[16,27,28] and osmium[17] corrole dimers (Table 2 and Figures 4 and 5).[29] The three classes of complexes all exhibit at least three reversible oxidations and one reversible reduction. Furthermore, for a given corrole ligand, the oxidation potentials were found to be nearly identical for the three metals, suggesting a lack of sensitivity to the nature of the metal−metal bonding and, hence, ligand-centered oxidation. The reduction potentials, in contrast, proved to be dramatically different for the three metals, being algebraically in the order Re > Ru > Os. The nearly 750-mV difference between the reduction potentials of Re and Os corrole dimers appears to be consistent with the thermodynamic ease of electron addition into the δ* orbital of the former and the difficulty of electron addition to the much higher-energy π* orbital of the latter.[30] For Ru, the reduction potential is not quite as negative as that for Os, in large part because an Ru−Ru π* LUMO is less relativistically destabilized than its Os counterpart. The electrochemical HOMO−LUMO gaps, i.e., the algebraic difference between the oxidation and reduction potentials, accordingly, are dramatically different for the three metals, increasing in the

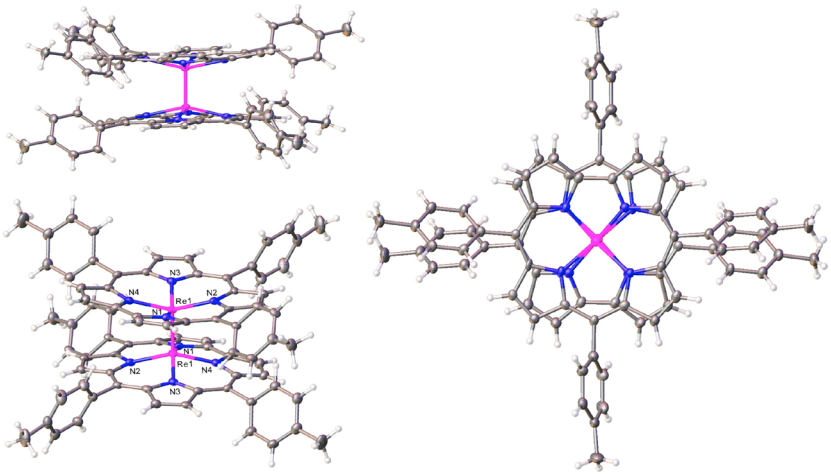

Figure 2. Thermal ellipsoid plots depicting three perspectives of {Re[T*p*MePC]}$_2$. Selected distances (Å): Re1−N1 2.010(8), Re1−N2 1.999(9), Re1−N3 2.030(9), Re1−N4 1.997(9), Re1−Re1 2.2364(6).

https://doi.org/10.1021/acs.inorgchem.1c00986
Inorg. Chem. 2021, 60, 8315−8321

Table 2. Spectroscopic and Electrochemical Properties of {Re[T*p*XPC]}$_2$, {Ru[T*p*XPC]}$_2$, and {Os[T*p*XPC]}$_2$: Soret and Q Band λ_{max} (nm) and $E_{1/2}$ Values (V vs SCE)

	λ_{max} (nm)									
complex	Soret	Q	$E_{1/2ox4}$	$E_{1/2ox3}$	$E_{1/2ox2}$	$E_{1/2ox1}$	$E_{1/2red1}$	$E_{1/2red2}$	ΔE	ref[a]
{Re[TPC]}$_2$	405	599		1.18	0.84	0.57	−0.54	*b*	1.11	tw
{Re[T*p*MePC]}$_2$	407	601		1.12	0.78	0.51	−0.55	*b*	1.06	tw
{Re[T*p*OMePC]}$_2$	408	602		1.09	0.74	0.49	−0.57	*b*	1.06	tw
{Ru[T*p*CF$_3$PC]}$_2$	328, 397	541		1.31	1.09	0.76	−0.63	−1.43	1.39	16
{Ru[TPC]}$_2$	328, 397	539	1.56	1.23	0.99	0.55	−0.86	−1.66	1.41	16
{Ru[T*p*MePC]}$_2$	329, 398	538	1.44	1.18	0.98	0.52	−0.85		1.37	16
{Ru[T*p*OMePC]}$_2$	329, 406	533	1.33	1.14	0.92	0.50	−0.86		1.36	16
{Os[T*p*CF$_3$PC]}$_2$	287, 407	583		1.28	1.01	0.79	−1.13	−1.54	1.92	17
{Os[TPC]}$_2$	287, 405	584		1.15	0.93	0.60	−1.29	−1.69	1.89	17
{Os[T*p*MePC]}$_2$	287, 407	584	1.35	1.09	0.88	0.55	−1.31	−1.72	1.86	17
{Os[T*p*OMePC]}$_2$	286, 407	585	1.28	1.05	0.85	0.54	−1.32	−1.73	1.86	17

[a]tw = this work. [b]A second reduction is partially discernible below −1.80 V, but it is not fully reversible at room temperature.

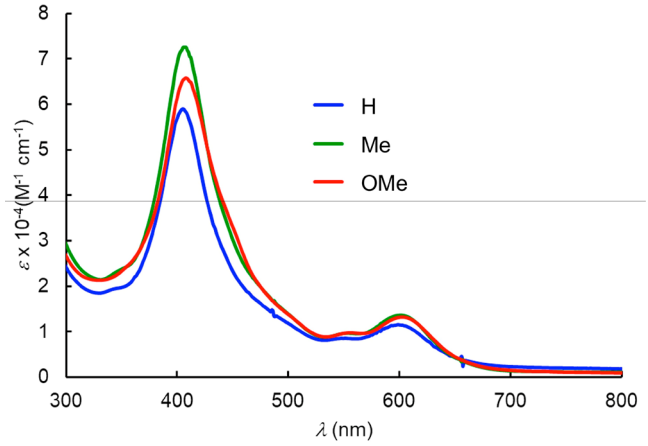

Figure 3. UV−vis spectra of {Re[T*p*XPC]}$_2$ in dichloromethane for X = H (blue), Me (green), and OMe (red).

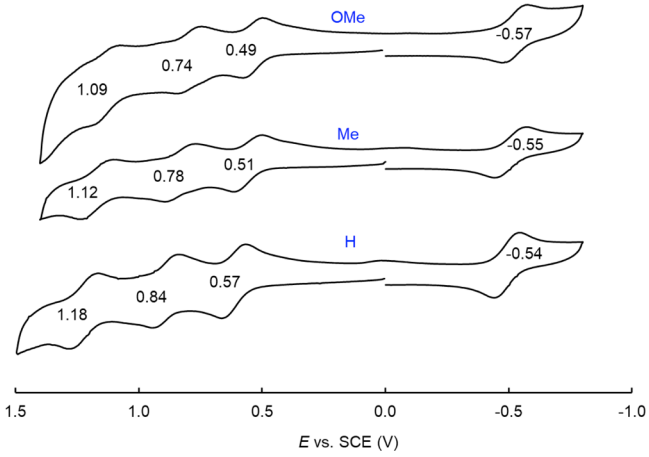

Figure 4. Cyclic voltammograms (V vs SCE) of {Re[T*p*XPC]}$_2$ for X = OMe, Me, and H in dichloromethane containing 0.1 M TBAP. Scan rate = 100 mV/s.

order Re < Ru < Os. Importantly, reversible reductions have rarely been observed for quadruple-bonded systems; the present study thus provides a unique measurement of the electrochemical HOMO−LUMO gap for such a system.

DFT Calculations. Scalar-relativistic DFT (OLYP/ZORA-STO-TZ2P) calculations[14] were undertaken on the ground

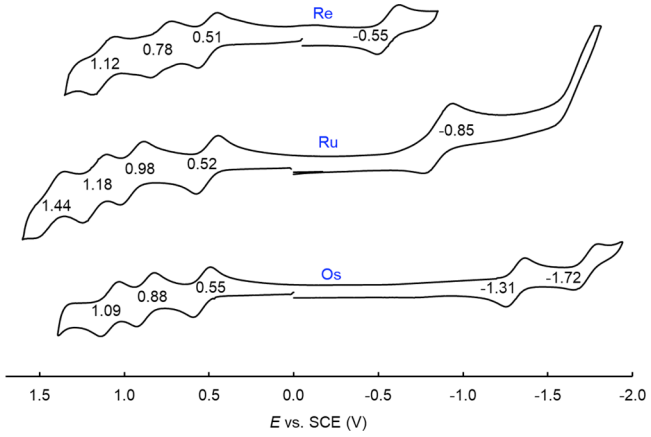

Figure 5. Comparison of the cyclic voltammograms of {M-[T*p*MePC]}$_2$ for M = Re, Ru, and Os.

state (C_{2h}, $S = 0$), lowest triplet state (C_2, $S = 1$), and cationic and anionic states (each C_2, $S = {}^1/_2$) of {Re[Cor]}$_2$. The calculations revealed a small HOMO−LUMO gap (0.26 eV) that closely matched vertical S_0−S_1 (0.28) and S_0−T_1 (0.24 eV) gaps obtained from time-dependent DFT calculations. The adiabatic S_0−T_1 gap proved smaller, about 0.10 eV, in part reflecting the rotation[31] of the two corrole rings relative to each other and the breaking of the δ bond. All of these energy gaps are considerably smaller than the electrochemical HOMO−LUMO gaps discussed above. That in itself, while interesting, is not particularly concerning, especially given the neglect of spin−orbit coupling in these calculations.

The major contribution of the calculations relates to the nature of the ionized states of {Re[Cor]}$_2$. While the calculated adiabatic ionization potential (5.88 eV) proved unremarkable (comparable to that of a variety of electron-rich porphyrin derivatives[32−36]), the electron affinity proved to be remarkably high (2.37 eV), indicating an unusually stable anionic state and in qualitative accord with the electrochemical data. Unsurprisingly, the spin density of the anionic state was found to correspond to electron addition to the δ^* orbital of the neutral dimer (Figure 6).[31] The nature of the cationic state proved to be more intriguing. For the {Re[Cor]}$_2$ cation, *each* Re atom was found to carry just over one electron spin, while the two corroles together were found to carry just over one minority spin. In other words, the overall electronic

https://doi.org/10.1021/acs.inorgchem.1c00986
Inorg. Chem. 2021, 60, 8315−8321

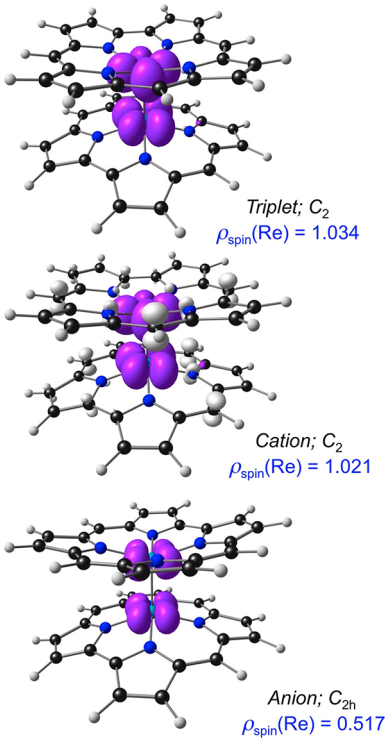

Figure 6. Spin-density profiles for the triplet, cationic, and anionic states of $\{Re[Cor]\}_2$. The majority and minority spin densities are shown in violet and ivory, respectively. Also shown are the effective point groups.

configuration appears to be $\delta(\uparrow)\delta^*(\uparrow)\pi(\downarrow)$, indicating a locally excited Re(III)−Re(III) axis antiferromagnetically coupled to a π radical spanning both corroles.[37−42] Such a description presumably reflects the close spacing of molecular orbitals in the HOMO region of the neutral C_{2h} dimer and a pseudo-Jahn−Teller distortion leading to a C_2 cation.[43] Thus, the electrochemical HOMO−LUMO gap does not quite correspond to the δ−δ^* orbital energy gap but may be legitimately regarded as an approximation to the latter.

CONCLUSION

Porphyrin ligands permitted the synthesis of a variety of highly stable complexes with metal−metal multiple bonds, in turn permitting a variety of unique physicochemical measurements.[9−12] Corroles now forcefully complement porphyrins in this role. The rhenium corrole dimers reported here are the first examples of quadruple-bonded metallocorrole dimers. The crystal structure of one such compound, $\{Re[TpMePC]\}_2$, revealed an Re−Re distance of 2.24 Å, which is essentially identical to the Os−Os distance in triple-bonded osmium corrole dimers. Electrochemical studies, on the other hand, revealed dramatically higher (i.e., less negative) reduction potentials relative to the Os compounds, reflecting electron addition to a δ^* LUMO in the Re case and to a π^*-based LUMO in the Os case. These studies also indicate unusually small electrochemical HOMO−LUMO gaps of 1.0−1.1 V in the Re case; these, surprisingly, rank among the first such measurements reported for quadruple-bonded transition-metal dimers, with porphyrin-type supporting ligands or otherwise.

EXPERIMENTAL SECTION

Materials. Free-base corroles were synthesized via the so-called water−methanol method.[20] All other reagents were purchased from Sigma-Aldrich (Merck) and used as received. Silica gel 60 (0.04−0.063 mm particle size, 230−400 mesh, Merck) was employed for flash chromatography. Silica gel 60 preparative thin-layer chromatographic plates (20 cm × 20 cm × 0.5 mm, Merck) were used for final purification of all complexes.

Instrumental Methods. UV−vis spectra were recorded on a Cary 8454 spectrophotometer. ^{1}H NMR spectra were recorded on a 400 MHz Bruker Avance III HD spectrometer (equipped with a 5-mm BB/^{1}H SmartProbe) at a temperature of 298 K in tetrahydrofuran (THF)-d_8 and referenced to residual THF protons at 3.48 and 2.37 ppm. High-resolution (HR) mass spectra were recorded (typically in the positive-ion mode) on a Thermo LTQ Orbitrap XL spectrometer equipped with an electrospray ION MAX source. Elemental analyses were performed by Atlantic Microlab, Inc.

Cyclic voltammetry was carried out at 298 K with an EG&G model 263A potentiostat having a three-electrode system: a glassy carbon working electrode, a platinum wire counterelectrode, and a standard calomel reference electrode (SCE). Tetra-*n*-butylammonium perchlorate, recrystallized twice from absolute ethanol and dried in a desiccator for at least two weeks, was used as the supporting electrolyte. Anhydrous CH_2Cl_2 (Sigma-Aldrich) was used as a solvent. The reference electrode was separated from the bulk solution by a fritted-glass bridge filled with a saturated AgCl/KCl mixture. The electrolyte solution was purged with argon for at least 2 min, and all measurements were carried out under an argon blanket. All potentials were referenced to the SCE.

General Procedure for the Synthesis of {Re[*Tp*XPC]}$_2$. To a two-necked 50-mL round-bottom flask were added the free-base corrole H_3[T*p*XPC], where X = H, CH_3, and OCH_3 (0.13 mmol), $Re_2(CO)_{10}$ (0.26 mmol, 173 mg), 2,6-lutidine (0.1 mL), 1,2-dichlorobenzene (10 mL), and a magnetic stirring bar. The contents of the mixture were deoxygenated with a constant flow of argon for 10 min and subsequently heated (refluxed) at 180 °C for 4 h, with constant stirring under argon. Completion of the reaction was indicated by disappearance of the Soret absorption of the free-base corrole. Upon cooling, the reaction mixture was loaded directly onto a silica-gel column with *n*-hexane as the mobile phase. 1,2-Dichlorobenzene was first removed by eluting with pure *n*-hexane. Subsequently, 1:3 *n*-hexane/dichloromethane mixtures were used to elute the red ReO corrole and then the green Re corrole dimer. The Re corrole dimers were further purified via preparative thin-layer chromatography using 1:2 *n*-hexane/dichloromethane, giving final yields of >10%. Analytical details for the new compounds are as follows.

{Re[TPC]}$_2$. Yield: 11 mg (11.65%). UV−vis [CH_2Cl_2; λ_{max}, nm (ε, $\times 10^{-4}$ M^{-1} cm^{-1})]: 405 (5.90), 548 (0.85), 599 (1.15). ^{1}H NMR (400 MHz, 25 °C, THF-d_8): δ 9.02 (d, 4H, $^3J_{HH}$ = 4.00 Hz, β-H), 8.86 (bs, 4H, β-H), 8.54 (d, 4H, $^3J_{HH}$ = 4.04 Hz, β-H), 8.37 (bs, 4H, β-H), 8.17 (bs, 4H, 5,15-*o*1-Ph), 8.07 (bs, 2H, 10-*o*1-Ph), 7.81 (m, 6H, 5,10,15-*o*2-Ph), 7.75 (bs, 6H, 5,10,15-*p*-Ph), 7.60 (m, 6H, 5,10,15-*m*1-Ph), 7.32 (m, 6H, 5,10,15-*m*2-Ph). Elem anal. found: C, 62.99; H, 3.62; N, 7.54. Calcd: C, 62.61; H, 3.27; N, 7.89. MS (ESI): M$^+$ = 1420.2979 (expt), 1420.2965 (calcd for $C_{74}H_{46}N_8Re_2$).

{Re[T*p*MePC]}$_2$. Yield: 10.2 mg (10.43%). UV−vis [CH_2Cl_2; λ_{max}, nm (ε, $\times 10^{-4}$ M^{-1} cm^{-1})]: 407 (7.25), 553 (0.96), 601 (1.36). ^{1}H NMR (400 MHz, 25 °C, THF-d_8): δ 9.02 (d, 2H, $^3J_{HH}$ = 9.00 Hz, 10-*o*1-Ph), 8.77 (d, 4H, $^3J_{HH}$ = 4.60 Hz, β-H), 8.64 (bs, 4H, 5,15-*o*1-Ph), 8.30 (d, 4H, $^3J_{HH}$ = 4.16 Hz, β-H), 8.19 (d, 4H, $^3J_{HH}$ = 4.56 Hz, β-H), 7.76 (d, 2H, $^3J_{HH}$ = 7.52 Hz, 10-*o*2-Ph), 7.63 (d, 4H, $^3J_{HH}$ = 4.16 Hz, β-H), 7.51 (bs, 4H, 5,15-*o*2-Ph), 7.23 (d, 6H, $^3J_{HH}$ = 7.04 Hz, 5,10,15-*m*1-Ph), 7.13 (m, 6H, 5,10,15-*m*2-Ph), 2.63 (s, 6H, 10-*p*CH_3), 2.59 (s, 12H, 5,15-*p*CH_3). Elem anal. found: C, 63.99; H, 3.68; N, 7.34. Calcd: C, 63.90; H, 3.89; N, 7.05. MS (ESI): M$^+$ = 1504.3918 (expt), 1504.3906 (calcd for $C_{80}H_{58}N_8Re_2$).

{Re[T*p*OMePC]}$_2$. Yield: 12 mg (11.53%). UV−vis [CH_2Cl_2; λ_{max}, nm (ε, $\times 10^{-4}$ M^{-1} cm^{-1})]: 408 (6.57), 554 (0.92), 602 (1.31). ^{1}H

https://doi.org/10.1021/acs.inorgchem.1c00986
Inorg. Chem. 2021, 60, 8315−8321

NMR (400 MHz, 25 °C, THF-d_8): δ 9.04 (d, 2H, $^3J_{HH}$ = 8.72 Hz, 10-*o*1-Ph), 8.80 (d, 4H, $^3J_{HH}$ = 4.56 Hz, β-H), 8.63 (bs, 4H, 5,15-*o*1-Ph), 8.29 (d, 4H, $^3J_{HH}$ = 4.16 Hz, β-H), 8.19 (d, 4H, $^3J_{HH}$ = 3.40 Hz, β-H), 7.60 (bs, 4H, 5,15-*o*2-Ph), 7.54 (d, 4H, $^3J_{HH}$ = 8.56 Hz, β-H), 7.28 (bs, 6H, Ph), 7.16−6.96 (m, 8H, Ph), 4.03 (s, 6H, 10-*p*OCH_3), 3.99 (s, 12H, 5,15-*p*OCH_3). Elem anal. found: C, 60.35; H, 3.72; N, 7.34. Calcd: C, 59.98; H, 3.61; N, 7.00. MS (ESI): M^+ = 1600.3617 (expt), 1600.3601 (calcd for $C_{80}H_{58}O_6N_8Re_2$).

Crystallization and Crystallography. X-ray data were collected on beamline 11.3.1 at the Advanced Light Source of Lawrence Berkeley National Laboratory, Berkeley, CA. The samples were mounted on MiTeGen kapton loops and placed in a 100(2) K nitrogen cold stream provided by an Oxford Cryostream 700 Plus low-temperature apparatus on the goniometer head of a Bruker D8 diffractometer equipped with a PHOTONII CPAD detector. Diffraction data were collected using synchrotron radiation monochromated with silicon (111) to a wavelength of 0.7749(1) Å. An approximate full-sphere of data was collected using 1° ω scans. The structures were solved by intrinsic phasing methods (*SHELXT*)[44] and refined by full-matrix least squares on F^2 (*SHELXL-2018*).[45] H atoms were geometrically calculated and refined as riding atoms.

Computational Methods. DFT calculations were carried out with the *ADF 2018* program system.[46] Relativistic effects were taken into account with the zeroth-order regular approximation (ZORA[47]) to the Dirac equation applied as a scalar correction. Specially optimized all-electron ZORA STO-TZ2P basis sets were used throughout. A variety of exchange-correlation functionals were tested; the results quoted are those for OLYP,[48,49] one of the better generalized gradient approximations that we have extensively used in our studies of metalloporphyrin-type compounds.[14]

■ ASSOCIATED CONTENT

Supporting Information

The Supporting Information is available free of charge at https://pubs.acs.org/doi/10.1021/acs.inorgchem.1c00986.

^{1}H NMR and HR-ESI-MS spectra and optimized Cartesian coordinates (PDF)

Accession Codes

CCDC 2073973 contains the supplementary crystallographic data for this paper. These data can be obtained free of charge via www.ccdc.cam.ac.uk/data_request/cif, or by emailing data_request@ccdc.cam.ac.uk, or by contacting The Cambridge Crystallographic Data Centre, 12 Union Road, Cambridge CB2 1EZ, UK; fax: +44 1223 336033.

■ AUTHOR INFORMATION

Corresponding Author

Abhik Ghosh − *Department of Chemistry, UiT—The Arctic University of Norway, N-9037 Tromsø, Norway;* orcid.org/0000-0003-1161-6364; Phone: +47 45476145; Email: abhik.ghosh@uit.no

Authors

Abraham B. Alemayehu − *Department of Chemistry, UiT—The Arctic University of Norway, N-9037 Tromsø, Norway;* orcid.org/0000-0003-0166-8937

Laura J. McCormick-McPherson − *Advanced Light Source, Lawrence Berkeley National Laboratory, Berkeley, California 94720-8229, United States;* orcid.org/0000-0002-6634-4717

Jeanet Conradie − *Department of Chemistry, UiT—The Arctic University of Norway, N-9037 Tromsø, Norway; Department of Chemistry, University of the Free State, Bloemfontein 9300, Republic of South Africa;* orcid.org/0000-0002-8120-6830

Complete contact information is available at: https://pubs.acs.org/10.1021/acs.inorgchem.1c00986

Notes

The authors declare no competing financial interest.

■ ACKNOWLEDGMENTS

This work was supported by Grant 262229 of the Research Council of Norway (AG) and Grants 129270 and 132504 of the South African National Research Foundation. This research used resources of the Advanced Light Source, which is a U.S. Department of Energy, Office of Science User Facility, under Contract DE-AC02-05CH11231.

■ REFERENCES

(1) Kuznetsov, V. G.; Koz'min, P. A. A study of the structure of (PyH)$HReCl_4$. *J. Struct. Chem.* **1963**, *4*, 49−55.

(2) Cotton, F. A.; Curtis, N. F.; Harris, C. B.; Johnson, B. F. G.; Lippard, S. J.; Mague, J. T.; Robinson, W. R.; Wood, J. S. Mononuclear and Polynuclear Chemistry of Rhenium (III): Its Pronounced Homophilicity. *Science* **1964**, *145*, 1305−1307.

(3) Cotton, F. A. Metal-Metal Bonding in $[Re_2X_8]^{2-}$ Ions and Other Metal Atom Clusters. *Inorg. Chem.* **1965**, *4*, 334−336.

(4) Cotton, F. A. Discovering and understanding multiple metal-to-metal bonds. *Acc. Chem. Res.* **1978**, *11*, 225−232.

(5) Trogler, W. C.; Gray, H. B. Electronic spectra and photochemistry of complexes containing quadruple metal-metal bonds. *Acc. Chem. Res.* **1978**, *11*, 232−239.

(6) Cotton, F. A.; Nocera, D. C. The Whole Story of the Two-Electron Bond, with the δ Bond as a Paradigm. *Acc. Chem. Res.* **2000**, *33*, 483−490.

(7) *Multiple bonds between metal atoms*; Cotton, F. A., Murillo, C. A., Walton, R. A., Eds.; Springer: New York, 2005; p 818 pp.

(8) Ndambuki, S.; Ziegler, T. An analysis of unsupported triple and quadruple metal−metal bonds between two homonuclear group 6 transition elements based on the combined natural orbitals for chemical valence and extended transition state method. *Int. J. Quantum Chem.* **2013**, *113*, 753−761.

(9) Collman, J. P.; Arnold, H. J. Multiple Metal-Metal Bonds in 4d and 5d Metal-Porphyrin Dimers. *Acc. Chem. Res.* **1993**, *26*, 586−592.

(10) Collman, J. P.; Garner, J. M.; Hembre, R. T.; Ha, Y. Relative Strength of 4d vs 5d δ-bonds: Rotational Barriers of Isostructural Molybdenum and Tungsten Porphyrin Dimers. *J. Am. Chem. Soc.* **1992**, *114*, 1292−1301.

(11) Collman, J. P.; Arnold, H. Delta bonds and rotational barriers in 4d and 5d metal-porphyrin dimers. *J. Cluster Sci.* **1994**, *5*, 37−66.

(12) Collman, J. P.; Boulatov, R. Heterodinuclear Transition-Metal Complexes with Multiple Metal−Metal Bonds. *Angew. Chem., Int. Ed.* **2002**, *41*, 3948−3961.

(13) Tait, C. D.; Garner, J. M.; Collman, J. P.; Sattelberger, A. P.; Woodruff, W. H. Vibrational characterization of multiply metal-metal bonded osmium, molybdenum, and rhenium porphyrin dimers. *J. Am. Chem. Soc.* **1989**, *111*, 9072−9077.

(14) Ghosh, A. Electronic Structure of Corrole Derivatives: Insights from Molecular Structures, Spectroscopy, Electrochemistry, and Quantum Chemical Calculations. *Chem. Rev.* **2017**, *117*, 3798−3881.

(15) Nardis, S.; Mandoj, F.; Stefanelli, M.; Paolesse, R. Metal complexes of corrole. *Coord. Chem. Rev.* **2019**, *388*, 360−405.

(16) Alemayehu, A. B.; Vazquez-Lima, H.; Gagnon, K. J.; Ghosh, A. Stepwise Deoxygenation of Nitrite as a Route to Two Families of Ruthenium Corroles: Group 8 Periodic Trends and Relativistic Effects. *Inorg. Chem.* **2017**, *56*, 5285−5294.

(17) Alemayehu, A. B.; McCormick, L. J.; Vazquez-Lima, H.; Ghosh, A. Relativistic Effects on a Metal−Metal Bond: Osmium Corrole Dimers. *Inorg. Chem.* **2019**, *58*, 2798−2806.

(18) Schweyen, P.; Brandhorst, K.; Hoffmann, M.; Wolfram, B.; Zaretzke, M.-K.; Bröring, M. Viking Helmet Corroles: Activating Inert Oxidometal Corroles. *Chem. - Eur. J.* **2017**, *23*, 13897−13900.
(19) Wasbotten, I. H.; Wondimagegn, T.; Ghosh, A. Electronic Absorption, Resonance Raman, and Electrochemical Studies of Planar and Saddled Copper(III) *meso*-Triarylcorroles. Highly Substituent-Sensitive Soret Bands as a Distinctive Feature of High-Valent Transition Metal Corroles. *J. Am. Chem. Soc.* **2002**, *124*, 8104−8116.
(20) Koszarna, B.; Gryko, D. T. Efficient Synthesis of *meso*-Substituted Corroles in a H_2O−MeOH Mixture. *J. Org. Chem.* **2006**, *71*, 3707−3717.
(21) Einrem, R. F.; Gagnon, K. J.; Alemayehu, A. B.; Ghosh, A. Metal-Ligand Misfits: Facile Access to Rhenium-Oxo Corroles by Oxidative Metalation. *Chem. - Eur. J.* **2016**, *22*, 517−520.
(22) Alemayehu, A. B.; Gagnon, K. J.; Terner, J.; Ghosh, A. Oxidative Metalation as a Route to Size-Mismatched Macrocyclic Complexes: Osmium Corroles. *Angew. Chem., Int. Ed.* **2014**, *53*, 14411−14414.
(23) Alemayehu, A. B.; Teat, S. J.; Borisov, S. M.; Ghosh, A. Rhenium-Imido Corroles. *Inorg. Chem.* **2020**, *59*, 6382−6389.
(24) Einrem, R. F.; Braband, H.; Fox, T.; Vazquez-Lima, H.; Alberto, R.; Ghosh, A. Synthesis and Molecular Structure of ^{99}Tc Corroles. *Chem. - Eur. J.* **2016**, *22*, 18747−18751.
(25) Pyykkö, P.; Riedel, S.; Patzschke, M. Triple-Bond Covalent Radii. *Chem. - Eur. J.* **2005**, *11*, 3511−3520.
(26) Alemayehu, A. B.; Gagnon, K. J.; Terner, J.; Ghosh, A. Oxidative Metalation as a Route to Size-Mismatched Macrocyclic Complexes: Osmium Corroles. *Angew. Chem., Int. Ed.* **2014**, *53*, 14411−14414.
(27) Simkhovich, L.; Luobeznova, I.; Goldberg, I.; Gross, Z. Mono- and Binuclear Ruthenium Corroles: Synthesis, Spectroscopy, Electrochemistry, and Structural Characterization. *Chem. - Eur. J.* **2003**, *9*, 201−208.
(28) Kadish, K. M.; Burdet, F.; Jerome, F.; Barbe, J.-M.; Ou, Z.; Shao, J.; Guilard, R. Synthesis, Physicochemical and Electrochemical Properties of Metal-Metal Bonded Ruthenium Corrole Homodimers. *J. Organomet. Chem.* **2002**, *652*, 69−76.
(29) Fang, Y.; Ou, Z.; Kadish, K. M. Electrochemistry of Corroles in Nonaqueous Media. *Chem. Rev.* **2017**, *117*, 3377−3419.
(30) Another interesting difference between Re and Os corrole dimers concerns their second reduction potentials. For the Re corrole dimers reported here, a second reduction is partially discernible below −1.80 V, but it is not quite reversible at room temperature. This observation translates to a gigantic difference of some 1300 mV between the first and second reduction potentials, compared to a value of only 130−380 mV for the corresponding quantity for Os corrole dimers. A possible explanation for the dramatic difference between the two metals is that, in the Re case, both reductions involve electron addition to the same δ^* orbital, whereas for Os, the reductions involve a pair of π^* orbitals. These details are currently under evaluation with UV−vis spectroelectrochemistry and additional DFT calculations.
(31) The two corrole rings are rotated approximately 135° relative to each other in the triplet and cation states or 45° relative to the C_{2h} ground state.
(32) Ghosh, A.; Almlöf, J. The ultraviolet photoelectron spectrum of free-base porphyrin revisited. The performance of local density functional theory. *Chem. Phys. Lett.* **1993**, *213*, 519−521.
(33) Ghosh, A. Substituent effects on valence ionization potentials of free base porphyrins: A local density functional study. *J. Am. Chem. Soc.* **1995**, *117*, 4691−4699.
(34) Ghosh, A. J. Theoretical Comparative Study of Free Base Porphyrin, Chlorin, Bacteriochlorin, and Isobacteriochlorin: Evaluation of the Potential Roles of *ab Initio* Hartree−Fock and Density Functional Theories in Hydroporphyrin Chemistry. *J. Phys. Chem. B* **1997**, *101*, 3290−3297.
(35) Ghosh, A.; Vangberg, T. Valence ionization potentials and cation radicals of prototype porphyrins. The remarkable performance of nonlocal density functional theory. *Theor. Chem. Acc.* **1997**, *97*, 143−149.
(36) Ghosh, A. First-Principles Quantum Chemical Studies of Porphyrins. *Acc. Chem. Res.* **1998**, *31*, 189−198.
(37) While the electronic structure may be different for substituted cations such as $\{Re[TPC]\}_2^+$, DFT has a long track record of describing noninnocent porphyrin and corrole[14,17] derivatives in a qualitatively correct manner.
(38) Ghosh, A.; Wondimagegn, T.; Parusel, A. B. J. Electronic Structure of Gallium, Copper, and Nickel Complexes of Corrole. High-Valent Transition Metal Centers Versus Noninnocent Ligands. *J. Am. Chem. Soc.* **2000**, *122*, 5100−5104.
(39) Ghosh, A.; Steene, E. High-valent transition metal centers and noninnocent ligands in metalloporphyrins and related molecules: a broad overview based on quantum chemical calculations. *JBIC, J. Biol. Inorg. Chem.* **2001**, *6*, 739−752.
(40) Ghosh, A. Transition metal spin state energetics and noninnocent systems: challenges for DFT in the bioinorganic arena. *JBIC, J. Biol. Inorg. Chem.* **2006**, *11*, 712−724.
(41) Thomas, K. E.; Vazquez-Lima, H.; Fang, Y.; Song, Y.; Gagnon, K. J.; Beavers, C. M.; Kadish, K. M.; Ghosh, A. Ligand Noninnocence in Coinage Metal Corroles: A Silver Knife-Edge. *Chem. - Eur. J.* **2015**, *21*, 16839−16847.
(42) Ganguly, S.; Ghosh, A. Seven Clues to Ligand Noninnocence: The Metallocorrole Paradigm. *Acc. Chem. Res.* **2019**, *52*, 2003−2014.
(43) Vangberg, T.; Lie, R.; Ghosh, A. Symmetry-Breaking Phenomena in Metalloporphyrin π-Cation Radicals. *J. Am. Chem. Soc.* **2002**, *124*, 8122−8130.
(44) Sheldrick, G. M. SHELXT - Integrated Space-Group and Crystal-Structure Determination. *Acta Crystallogr., Sect. A: Found. Adv.* **2015**, *A71*, 3−8.
(45) Sheldrick, G. M. Crystal Structure Refinement with SHELXL. *Acta Crystallogr., Sect. C: Struct. Chem.* **2015**, *C71*, 3−8.
(46) te Velde, G.; Bickelhaupt, F. M.; Baerends, E. J.; Fonseca Guerra, C.; van Gisbergen, S. J. A.; Snijders, J. G.; Ziegler, T. Chemistry with ADF. *J. Comput. Chem.* **2001**, *22*, 931−967.
(47) van Lenthe, E.; Ehlers, A.; Baerends, E. J. Geometry optimizations in the zero order regular approximation for relativistic effects. *J. Chem. Phys.* **1999**, *110*, 8943−8953.
(48) Handy, N. C.; Cohen, A. J. Left-right correlation energy. *Mol. Phys.* **2001**, *99*, 403−412.
(49) Lee, C.; Yang, W.; Parr, R. G. Development of the Colle-Salvetti correlation-energy formula into a functional of the electron density. *Phys. Rev. B: Condens. Matter Mater. Phys.* **1988**, *37*, 785−789.

https://doi.org/10.1021/acs.inorgchem.1c00986
Inorg. Chem. 2021, 60, 8315−8321